Convergence of the SMI and the Diagonally Loaded SMI Algorithms with Weak Interference

MATTHEW W. GANZ, MEMBER, IEEE, RANDOLPH L. MOSES, MEMBER, IEEE, AND SANFORD L. WILSON

Abstract—**The sample matrix inversion (SMI) algorithm is commonly used in adaptive arrays since it offers rapid convergence to the maximum signal-to-interference-plus-noise ratio (SINR) solution. However, in some applications, such as digital communications or satellite television communications, other measures of performance such as the signal-to-interference ratio (SIR) may be equally important. In this paper approximations are derived for the power levels at the output of an adaptive array that uses the diagonally loaded SMI algorithm. Diagonal loading is a technique where the diagonal of the covariance matrix is augmented with a positive or negative constant prior to inversion. We examine how SINR and SIR at the array output vary with the number of samples taken when the input signals are continuous wave. It is shown that positive loading produces more rapid convergence with a reduction in output SIR. Negative loading provides an improved SIR level, but it is shown that the output power levels are erratic and slow to converge. Simulation results are given which verify the theoretical predictions.**

I. Introduction

An adaptive array is a phased array antenna in which the element weights are adaptively controlled. Adaptive arrays can be used to protect radar and communication systems from interference by steering antenna pattern nulls in the directions of undesired signals. The weights are controlled by an algorithm that maximizes some performance measure. The most often used performance measure is the signal-to-interference-plus-noise ratio (SINR). The weights that produce the maximum SINR solution are often called the Wiener weights because they solve the Wiener–Hopf equation [1]. In digital adaptive arrays the covariance matrix, which appears in the Wiener weight solution, is typically estimated by a maximum likelihood estimate called the sample covariance matrix [2]. These arrays are often referred to as sample matrix inversion (SMI) arrays.

Most of the past studies of adaptive array performance have used the SINR as the measure of system performance. However, as is shown by Gupta in [3] and Ganz and Compton in [4] and [5], SINR is not always the best measure of system performance, especially when the interference is coherent or non-Gaussian. Other solutions have been proposed which maximize other performance measures. For instance, Gupta [3] has shown that if a small term is subtracted from each diagonal element of the sample covariance matrix prior to inversion, the resulting weights will produce deeper nulls on weak interfering signals. This technique can be useful in applications such as television reception from geosynchronous satellites, where weak interference from adjacent satellites can produce ghosts that are unacceptable to viewers. Alternatively, Gabriel [6], Cox *et al.* [7], Carlson [8], and others have suggested adding a small term to each diagonal element of the covariance matrix prior to inversion; this has the effect of increasing the convergence rate of the weights at the cost of reduced suppression of weak interference. We refer to the augmentation of the diagonal terms of the covariance matrix with a negative constant as negative diagonal loading and we refer to augmentation of the diagonal terms with a positive constant as positive diagonal loading.

Since the Wiener weights produce the maximum array output SINR, either positive or negative diagonal loading produces suboptimal solutions as measured by SINR. The primary advantage of positive diagonal loading is faster weight convergence (albeit to a suboptimal solution). As shown in [6] and [8], the sidelobe level of a pattern obtained with a small number of samples is generally lower and more stable when positive loading is used. Negative diagonal loading produces a suboptimal SINR value but it produces a signal-to-interference ratio (SIR) higher than that of unloaded SMI [3].

Reed, Mallet, and Brennan, in a well-known paper [2], show that the SINR at the output of an array using the (non-diagonally loaded) SMI algorithm converges to within 3 dB of its optimum value more than half the time when more than $2N-3$ samples are taken (where N is the number of antenna elements). This result is derived under the assumptions that the interfering signals at the array input are Gaussian and the desired signal is not included in the sample covariance matrix. Boroson [9] extends these results and considers the effects of the desired signal data and steering vector errors. Boroson shows that convergence can be much slower when the desired signal is included in the sample covariance matrix.

In this paper we develop large-sample expressions for the desired, interfering, and noise power levels at the output of an SMI array as a function of the number of samples used in estimating the covariance matrix. These expressions are simple

Manuscript received September 29, 1988; revised March 22, 1989. This work was supported in part by the Department of the Navy under Air Force Contract F19628-85-C-0002, and in part by NASA Lewis Research Center Grant NAG3-536.

M. W. Ganz and S. L. Wilson are with MIT Lincoln Laboratory, P.O. Box 73, Lexington, MA 02173.

R. L. Moses is with the Department of Electrical Engineering, The Ohio State University, Columbus, OH 43210.

IEEE Log Number 8930395.

and easily programmed on a computer. As a result they can be used instead of tedious and computationally expensive Monte Carlo simulations to obtain array performance estimates. In addition, since these expressions provide closed-form performance measures as a function of array and scenario parameters, one can quickly see the effects of these parameters on system performance.

The results we derive are used to examine the expected value of the SINR and SIR at the output of SMI arrays with and without diagonal loading. We show that positive loading tends to reduce the null depth on weak interfering signals while it decreases the convergence time. Conversely, negative loading tends to increase the null depth on weak interfering signals while increasing convergence time. We show that, with negative loading, it can often take thousands of samples before the SIR at the array output approaches the theoretical predictions based upon SMI with the true (i.e., nonsampled) covariance matrix. We also show that the output SINR and SIR with negative diagonal loading are erratic until a relatively large number of samples are taken. We present several examples that show how the theoretical predictions compare with simulated data and discuss the limitations of the theoretical results.

The next section contains the theoretical predictions of the system performance. Section III presents the example calculations and simulation results. Finally, Section IV contains the conclusions.

II. Analysis

Consider an N-element adaptive array with isotropic elements spaced one-half wavelength apart. We assume a continuous wave (CW) desired signal in an environment of J CW jammers. The desired signal and interfering signals are assumed to be of the form

$$d(t) = A_d \exp[j(\omega_d t + \Psi_d)], \tag{1}$$

$$i_\alpha(t) = A_\alpha \exp[j(\omega_\alpha t + \Psi_\alpha)], \qquad \alpha = 1, 2, \cdots, J \tag{2}$$

where A_d and A_α are the desired and interfering signal amplitudes and Ψ_d and the Ψ_α are the signal phases. Ψ_d and Ψ_α are independent and identically distributed uniformly on $[0, 2\pi]$. We assume that independent thermal noise signals, each with power σ^2, are present on each element.

Fig. 1 shows a typical linear array geometry.[1] The desired signal arrives from an angle θ_d and the αth interfering signal arrives from an angle θ_α. We assume that $\omega_d \approx \omega_\alpha$ so that the element-to-element phase shifts for the desired and interfering signals are given by $\phi_d = \pi \sin \theta_d$ and $\phi_\alpha = \pi \sin \theta_\alpha$, respectively.

We define the signals at the element inputs by $x_1, \cdots, x_N$, and we define the input signal vector by $\mathbf{X} = [x_1, \cdots, x_N]^T$, where T denotes the transpose. Note that we use boldface type for vectors or matrices and subscripted normal type to indicate vector or matrix elements.

The (true) diagonally loaded covariance matrix is defined by

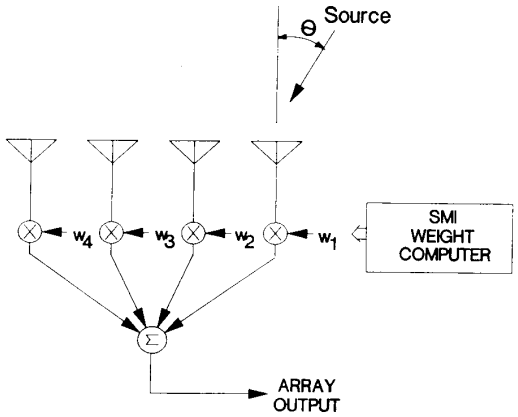

Fig. 1. A four-element SMI adaptive array.

$$\mathbf{R} = E[\mathbf{X}^*\mathbf{X}^T] + F\mathbf{I}, \tag{3}$$

where $E[\cdot]$ denotes expectation, the asterisk indicates complex conjugate, and $\mathbf{I}$ is the $N \times N$ identity matrix. The (scalar) parameter F denotes the amount of diagonal loading. If $F = 0$, no diagonal loading is present, and (3) gives the standard covariance matrix. Note that F can be positive or negative, but F must be greater than $-\sigma^2$ for the covariance matrix to be positive definite (and thus invertible). In general, values of F very close to $-\sigma^2$ should be avoided to ensure numerical stability during matrix inversion.

The corresponding diagonally loaded array weight vector is given by

$$\mathbf{W} = \mathbf{R}^{-1}\mathbf{S}, \tag{4}$$

where $\mathbf{S}$ is the steering vector which, for identical linearly spaced elements, is given by $\mathbf{S} = [1, e^{j\phi_d}, \cdots, e^{(N-1)j\phi_d}]^T$. When $F = 0$, $\mathbf{W}$ is the maximum SINR (Wiener) weight vector.

In the SMI algorithm the covariance matrix is estimated by sampling the incoming data. The diagonally loaded sample covariance matrix $\hat{\mathbf{R}}$ is given by

$$\hat{\mathbf{R}} = \frac{1}{K}\sum_{m=1}^{K}[\mathbf{X}^*(m)\mathbf{X}^T(m)] + F\mathbf{I}, \tag{5}$$

where $\mathbf{X}(m)$ is the mth snapshot of the signal vector. The kth element of $\mathbf{X}(m)$ is given by

$$x_k(m) = d(m)e^{j\phi_d(k-1)} + \sum_{\alpha=1}^{J} i_\alpha(m)e^{j\phi_\alpha(k-1)} + n_k(m), \tag{6}$$

where $d(m)$ and $i_\alpha(m)$ are the samples of the desired and interfering signals on the first elements. We assume that the sampling instants are chosen asynchronously with the carriers and modulation so that the $d(m)$ and $i(m)$ are given by

$$d(m) = A_d e^{j(\psi_d(m))}, \quad i_\alpha(m) = A_\alpha e^{j(\psi_\alpha(m))}, \tag{7}$$

where $\psi_d(m)$ and $\psi_\alpha(m)$ are independent and identically dis-

[1] For ease of understanding, we present our results for a simple array geometry with CW desired and interference signals. However, most of the derivation in this paper applies to more complicated array geometries and signal scenarios as well; see the comments below (27).

tributed random variables uniformly distributed on $[0, 2\pi]$. $n_k(m)$, the thermal noise on element k at the mth sample time, is Gaussian distributed as $N(0, \sigma^2)$.

The klth element of the true covariance matrix is obtained by evaluating the expectation

$$R_{kl} = E\{x_k^* x_l + F\delta_{kl}\}, \tag{8}$$

$$= |A_d|^2 e^{j\phi_d(l-k)} + \sum_{\alpha=1}^{J} |A_\alpha|^2 e^{j\phi_\alpha(l-k)} + \sigma^2\delta_{kl} + F\delta_{kl}, \tag{9}$$

$$\triangleq (\mathbf{R}_d)_{kl} + (\mathbf{R}_i)_{kl} + (\mathbf{R}_n)_{kl} + (\mathbf{R}_F)_{kl}, \tag{10}$$

where $\mathbf{R}_d$, $\mathbf{R}_i$, $\mathbf{R}_n$, $\mathbf{R}_F$ are, respectively, the desired, interference, noise, and diagonal loading parts of the covariance matrix and δ_{kl} is the Kronecker delta.

We define the error covariance matrix $\tilde{\mathbf{R}}$ to be the difference between the true covariance matrix and the sample covariance matrix. That is,

$$\tilde{\mathbf{R}} = \mathbf{R} - \hat{\mathbf{R}}. \tag{11}$$

The sample weights are then given by

$$\hat{\mathbf{W}} = \hat{\mathbf{R}}^{-1}\mathbf{S}. \tag{12}$$

Likewise, we can define the error weight vector by

$$\tilde{\mathbf{W}} = \mathbf{W} - \hat{\mathbf{W}}. \tag{13}$$

The inverse of the sample covariance matrix is given by

$$\hat{\mathbf{R}}^{-1} = (\mathbf{R} - \tilde{\mathbf{R}})^{-1} = [\mathbf{I} - \mathbf{R}^{-1}\tilde{\mathbf{R}}]^{-1}\mathbf{R}^{-1}. \tag{14}$$

We expand the bracketed term as [10, p. 301]

$$[\mathbf{I} - \mathbf{R}^{-1}\tilde{\mathbf{R}}]^{-1} = \sum_{i=0}^{\infty} (\mathbf{R}^{-1}\tilde{\mathbf{R}})^i = \mathbf{I} + \mathbf{R}^{-1}\tilde{\mathbf{R}} + \cdots. \tag{15}$$

It will be shown that the standard deviation of the elements of $\mathbf{R}^{-1}\tilde{\mathbf{R}}$ is inversely proportional to the square root of the number of data samples, that is, they are $O(1/\sqrt{K})$. It follows that the elements of $(\mathbf{R}^{-1}\tilde{\mathbf{R}})^i$ are $O(K^{-i/2})$. Thus, for large K, the matrix $[\mathbf{I} - \mathbf{R}^{-1}\tilde{\mathbf{R}}]^{-1}$ is well approximated by its first two terms. With this approximation we have

$$\hat{\mathbf{R}}^{-1} \approx [\mathbf{I} + \mathbf{R}^{-1}\tilde{\mathbf{R}}]\mathbf{R}^{-1}. \tag{16}$$

Strictly speaking, the expansion in (15) is valid only when the following inequality is satisfied

$$\|\mathbf{R}^{-1}\tilde{\mathbf{R}}\| < 1, \tag{17}$$

where $\|\cdot\|$ is any valid matrix norm used to evaluate the closeness of approximation in (16); see [10, p. 290]. We will return to this point later.

From (4), (12), (13), and (16) we find that the weight error vector is given by

$$\tilde{\mathbf{W}} = \mathbf{R}^{-1}\mathbf{S} - \hat{\mathbf{R}}^{-1}\mathbf{S} = -\mathbf{R}^{-1}\tilde{\mathbf{R}}\mathbf{W}. \tag{18}$$

The array output signal obtained with the sample weights is

$$s = \hat{\mathbf{W}}^T\mathbf{X}. \tag{19}$$

The average power at the array output is given by

$$P = \frac{1}{2}E[s^* s], \tag{20}$$

$$= \frac{1}{2}E[\hat{\mathbf{W}}^\dagger \mathbf{X}^* \mathbf{X}^T \hat{\mathbf{W}}], \tag{21}$$

$$= \frac{1}{2}\mathbf{W}^\dagger E[\mathbf{X}^*\mathbf{X}^T]\mathbf{W} + \frac{1}{2}E[\tilde{\mathbf{W}}^\dagger \mathbf{X}^*\mathbf{X}^T\tilde{\mathbf{W}}], \tag{22}$$

where the dagger indicates Hermitian transpose and we have assumed that $E[\tilde{\mathbf{W}}] = 0$.

The first term in (22) is the power that we would have at the array output with an infinite number of samples. To evaluate the second term in (22) we must determine $E[\tilde{w}_k^* \tilde{w}_l]$, which involves the fourth-order moments of the input signal. This term introduces the effects of finite sampling. We can expand the second term in (22) and then separate P into its desired (P_d), interfering (P_i), and noise (P_n) components as

$$P_d = \frac{1}{2}\mathbf{W}^\dagger \mathbf{R}_d \mathbf{W} + \frac{1}{2}\sum_{k=1}^{N}\sum_{l=1}^{N} E[\tilde{w}_k^* \tilde{w}_l](\mathbf{R}_d)_{kl}, \tag{23}$$

$$P_i = \frac{1}{2}\mathbf{W}^\dagger \mathbf{R}_i \mathbf{W} + \frac{1}{2}\sum_{k=1}^{N}\sum_{l=1}^{N} E[\tilde{w}_k^* \tilde{w}_l](\mathbf{R}_i)_{kl}, \tag{24}$$

$$P_n = \frac{1}{2}\mathbf{W}^\dagger \mathbf{R}_n \mathbf{W} + \frac{1}{2}\sum_{k=1}^{N}\sum_{l=1}^{N} E[\tilde{w}_k^* \tilde{w}_l](\mathbf{R}_n)_{kl}. \tag{25}$$

In order to evaluate these expressions we must calculate $E[\tilde{w}_k^* \tilde{w}_l]$, the covariance of the weight errors. From (18) this expectation is given in matrix form by

$$E[\tilde{\mathbf{W}}\tilde{\mathbf{W}}^\dagger] = E[\mathbf{R}^{-1}\tilde{\mathbf{R}}\mathbf{W}\mathbf{W}^\dagger\tilde{\mathbf{R}}^\dagger(\mathbf{R}^{-1})^\dagger]. \tag{26}$$

An expression for the ijth element $E[\tilde{w}_i^* \tilde{w}_j]$ is given by

$$E[\tilde{w}_i^* \tilde{w}_j] = \sum_{s=1}^{N}\sum_{t=1}^{N}\sum_{k=1}^{N}\sum_{l=1}^{N} (\mathbf{R}^{-1})_{is}^* (\mathbf{R}^{-1})_{jk} w_t^* w_l E[\tilde{R}_{st}^* \tilde{R}_{kl}]. \tag{27}$$

Note that (27) was derived without any assumptions about array geometry or signal scenario. Thus, this equation holds for a large class of arrays. The particular array assumptions are all contained in the particular form of $E[\tilde{R}_{st}^* \tilde{R}_{kl}]$. For the linear array of identical elements with CW signals this expectation is given by [11]

$$E[\tilde{R}_{st}^* \tilde{R}_{kl}] = \frac{1}{K}\left\{ \sigma^4\delta_{sk}\delta_{tl} + \sum_{\alpha=1}^{J}\sum_{\substack{\beta=1 \\ \alpha\neq\beta}}^{J} |A_\alpha|^2 |A_\beta|^2 e^{j\phi_\alpha(s-k)} e^{j\phi_\beta(l-t)} + \sum_{\alpha=1}^{J} |A_d|^2 |A_\alpha|^2 [e^{j\phi_d(s-k)} e^{j\phi_\alpha(l-t)} + e^{j\phi_d(l-t)} e^{j\phi_\alpha(s-k)}] + \sum_{\alpha=1}^{J} \sigma^2 |A_\alpha|^2 [\delta_{tl} e^{j\phi_\alpha(s-k)} + \delta_{sk} e^{j\phi_\alpha(l-t)}] + \sigma^2 |A_d|^2 [\delta_{tl} e^{j\phi_d(s-k)} + \delta_{sk} e^{j\phi_d(l-t)}] \right\}. \tag{28}$$

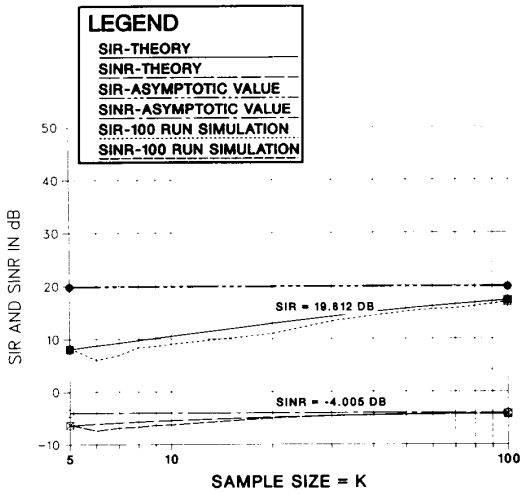

Fig. 2. SINR and SIR versus K, the number of samples, input SNR = −10 dB, input INR = −10 dB, no diagonal loading.

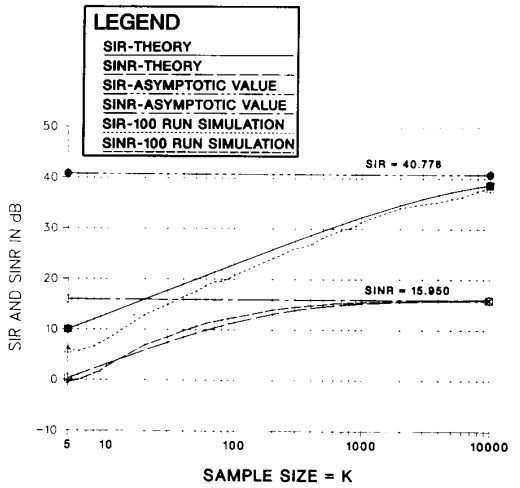

Fig. 3. SINR and SIR versus K, the number of samples, input SNR = 10 dB, input INR = 0 dB, no diagonal loading.

Equation (28) shows that the variance of $\tilde{\mathbf{R}}$ is proportional to $1/K$, so its standard deviation is $O(1/\sqrt{K})$, as we assumed earlier.

By substituting (28) into (27), and this result into (23)–(25), we obtain expressions for the expected values of the output powers as a function of data sample size K. These powers can then be used to compute figures of merit for the array. The two figures of merit that we consider are the signal-to-interference ratio and the SINR defined by

$$\text{SIR} = \frac{P_d}{P_i}, \quad \text{SINR} = \frac{P_d}{P_i + P_n}. \tag{29}$$

III. Results

In this section we look at several examples which illustrate the results derived above. We first examine a case where we have two weak signals incident upon a four-element array. In this case we have a desired signal with a −10 dB (per element) signal-to-noise ratio incident from the broadside direction ($\theta_d = 0°$) and an interfering signal with a −10 dB interference-to-noise ratio (INR) arriving from $\theta_i = 35°$. Fig. 2 shows the SINR and SIR as functions of K, the number of samples taken. The curves in this plot show the asymptotic SINR and SIR values, i.e., the values obtained using the true covariance matrix, or equivalently, the values obtained from the sample covariance matrix as the number of samples approaches infinity. Also shown are the values predicted by the analysis of the previous section, and the averaged results from 100 computer simulation runs. We note that the SINR converges quickly within 3 dB of its asymptotic value while SIR converges much more slowly. From these figures we see excellent agreement between the theoretical and simulation results. We note that the approximation given in (16) is good for the case shown in this example since the signals incident upon the array are weak.

As a second example we show SIR and SINR curves for a case where we have increased the SNR to 10 dB and increased the INR to 0 dB. The results for this case are shown in Fig. 3. From this figure we again see close agreement between the predicted and simulated results; however, the simulation results do not track the predictions quite as well in this case. We also note that convergence of the SINR curves to within 3 dB of the asymptotic value takes approximately 200 samples. This value is much larger than $2N - 3 = 5$ and verifies Boroson's results that SMI convergence is slowed by the addition of the desired signal in the covariance matrix [9].

TABLE I
Approximate Number of Samples Required for (17) to be Satisfied

SNR	INR	K REQUIRED
−10	−20	14
0	−10	17
10	0	36
20	10	220

In order to determine the region where the approximation (16) is good we examine how the Euclidean norm [10] of $\mathbf{R}^{-1}\tilde{\mathbf{R}}$ varies with K and INR. We consider several cases where we have different input signal levels. In each case we have an input SIR of 10 dB. We determine the minimum value of K required for (16) to be satisfied using a Monte Carlo simulation. The results are shown in Table I. This table shows that, as the signal strengths increase, the minimum value of K where we expect good agreement between theory and simulation increases. Here, 100 trials were averaged for each value given in the table. The signal arrival angles were the same as those used for Figs. 2 and 3.

From Table I we see that, for the case shown in Fig. 3, we do not expect good performance until K is greater than 36. From this figure we see that, for $K > 36$, the predicted and simulated SINR curves are within about 2 dB of each other and the predicted and simulated SIR curves are within about 3 dB.

We next consider the effect of diagonal loading of the sample covariance matrix. We consider the effects of both positive

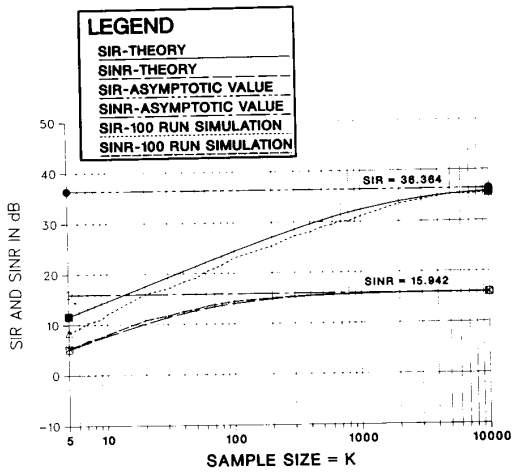

Fig. 4. SINR and SIR versus K, the number of samples, input SNR = 10 dB, input INR = 0 dB, $F = \sigma^2$ (positive diagonal loading).

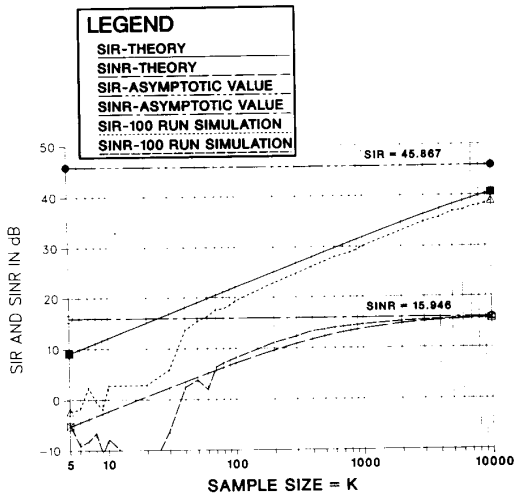

Fig. 5. SINR and SIR versus K, the number of samples, input SNR = 10 dB, input INR = 0 dB, $F = -0.5\sigma^2$ (negative diagonal loading).

and negative loading. Fig. 4 shows the effects when 3 dB of positive loading is added to the covariance matrix (i.e., σ^2 is added to each diagonal element of $\hat{\mathbf{R}}$). All the other parameters are unchanged from the case shown in Fig. 3. We see from this figure that the SIR asymptote is approximately 5.8 dB lower than it was without diagonal loading but the SINR asymptote is only negligibly lower. We see that the positive loading has decreased the number of samples required for convergence of the SINR curves to their asymptotic value. In this case the predicted and simulated curves for both SINR and SIR are within approximately 2 dB to each other for $K > 36$.

Finally we consider the effects of negative diagonal loading. Fig. 5 shows the results when $0.5\sigma^2$ is subtracted from each term of the covariance matrix. Again the signal scenario is that of Fig. 3. From Fig. 5 we see that the SINR asymptote is again only negligibly lower than that achieved without the loading, but the SIR asymptote is 5.9 dB higher. This is the result shown by Gupta in [3] and is the primary motivation for negative diagonal loading. We notice that, although a better SIR is achieved with the negative loading, convergence to the asymptotic value is slower than for the unloaded case. Again we see good tracking between the theoretical and simulated results. However, we found that in all our simulations with negative loading the output SIR and SINR are quite erratic when a small number of samples are taken. This is because the *variance* of the output powers are large for small sample lengths. This is evidenced by the jagged curves in Fig. 5 for K values below about 50; the average of 100 computer simulations was not enough to obtain an accurate statistical average of the powers for these small values of K.

IV. Conclusion

In this paper we have examined how the standard and diagonally loaded SMI algorithms converge with CW input signals as the number of samples taken increases. We developed approximations for the weight covariance and the output power levels from the array as a function of the number of samples taken. We presented several examples that show the performance for several signal scenarios and loading levels. We showed that, although SINR converges to within 3 dB of the asymptotic value within approximately a few hundred samples, SIR can converge much more slowly. This is especially true when negative diagonal loading is applied to the sample covariance matrix. The results derived here can be used to predict the number of samples required for SIR convergence without resorting to simulation. These results were shown to hold best when the incoming signals are weak or when the number of samples taken is large.

References

[1] B. Widrow, P. E. Mantey, L. J. Griffiths, and B. B. Goode, "Adaptive antenna systems," *Proc. IEEE*, vol. 55, no. 12, pp. 2143–2159, Dec. 1967.

[2] I. S. Reed, J. D. Mallett, and L. E. Brennan, "Rapid convergence rate in adaptive arrays," *IEEE Trans. Aerospace Electron. Syst.*, vol. AES-10, no. 5, pp. 853–862, Nov. 1974.

[3] I. J. Gupta, "SMI adaptive antenna arrays for weak interfering signals," *IEEE Trans. Antennas Propagat.*, vol. AP-34, no. 10, pp. 1237–1242, Oct. 1986.

[4] M. W. Ganz and R. T. Compton, Jr., "Protection of PSK communication systems with adaptive arrays," *IEEE Trans. Aerospace Electron. Syst.*, vol. AES-23, no. 4, pp. 528–536, July 1987.

[5] ——, "Protection of a narrow-band BPSK communication system with an adaptive array," *IEEE Trans. Commun.*, vol. COM-23, no. 10, pp. 1005–1011, October 1987.
[6] W. F. Gabriel, "Using spectral estimation techniques in adaptive processing antenna systems," *IEEE Trans. Antennas Propagat.*, vol. AP-34, no. 3, pp. 291–300, Mar. 1986.
[7] H. Cox, R. M. Zeskind, and M. N. Owen, "Robust adaptive beamforming," *IEEE Trans. Acoust. Speech, Signal Processing*, vol. ASSP-25, no. 10, pp. 1365–1376, Oct. 1987.
[8] B. D. Carlson, "Covariance matrix estimation errors and diagonal loading in adaptive arrays," *IEEE Trans. Aerospace Electron. Syst.*, vol. AES-24, no. 4, pp. 397–401, July 1988.
[9] D. M. Boroson, "Sample size considerations for adaptive arrays," *IEEE Trans. Aerospace Electron. Syst.*, vol. AES-16, no. 4, pp. 446–451, July 1980.
[10] R. A. Horn and C. A. Johnson, *Matrix Analysis*. Cambridge, England: Cambridge Univ. Press, 1985.
[11] M. W. Ganz, R. L. Moses, and S. L. Wilson, "Convergence of the diagonally loaded SMI algorithm," MIT Lincoln Lab., Lexington, MA, Tech. Rep. RST-40, Apr. 1989.

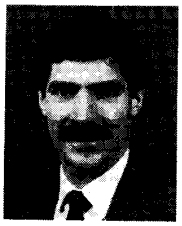

Matthew W. Ganz (S'82–M'85) was born in Toledo, OH, on March 18, 1959. He received the B.S., M.S., and Ph.D. degrees in electrical engineering from The Ohio State University, Columbus, in 1981, 1982, and 1986, respectively.

In 1980–1982 and 1985–1986 he was a University Fellow, a Graduate Research Associate, and a Postdoctoral Research Associate at The Ohio State University ElectroScience Laboratory where he studied communications and radar applications of adaptive antenna systems. From 1982–1984 he was an Associate Engineer in the Space Department of The Johns Hopkins University Applied Physics Laboratory. There he worked primarily on satellite communication and tracking systems. He is currently a Member of the Technical Staff in the Radar Systems Group at MIT Lincoln Laboratory, Lexington, MA, where he is working on radar applications of adaptive arrays.

Dr. Ganz is a member of Tau Beta Pi, Eta Kappa Nu, and Sigma Xi.

Randolph L. Moses (S'78–M'84) received the B.S., M.S., and Ph.D. degrees in electrical engineering from Virginia Polytechnic Institute and State University Blacksburg, in 1979, 1980, and 1984, respectively.

During the summer of 1983 he was an SCEEE Summer Faculty Research Fellow at Rome Air Development Center, Rome, NY. From 1984 to 1985 he was with the Eindhoven University of Technology, Eindhoven, The Netherlands, as a NATO Postdoctoral Fellow. Since 1985 he has been an Assistant Professor in the Department of Electrical Engineering, The Ohio State University. His research interests are in digital signal processing, and include parametric time series analysis, system identification, and model reduction.

Dr. Moses is a member of Eta Kappa Nu, Tau Beta Pi, Phi Kappa Phi, and Sigma Xi.

Sanford L. Wilson was born in Coral Gables, FL, on August 4, 1958. He received the B.S. degree in physics and the B.S. degree in mathematics in 1981, the M.S. degree in physics in 1982 from the Georgia Institute of Technology, Atlanta, and the Ph.D. degree from the University of Texas, Austin, in 1987.

He is currently a member of the Technical Staff in the Radar Systems Group at the MIT Lincoln Laboratory, Lexington, MA, where he is working on clutter rejection techniques and detection theory.